Journal of Pharmaceutical and Biomedical Analysis 283 (2027) 117740

Contents lists available at ScienceDirect

Journal of Pharmaceutical and Biomedical Analysis

journal homepage: www.journals.elsevier.com/journal-of-pharmaceutical-and-biomedical-analysis

Peak integration errors and analyst interaction in pharmaceutical quality control using LC–UV

Martin Enmark [a], Eivor Örnskov [b], Patrik Forssén [a], Jörgen Samuelsson [a], Torgny Fornstedt [a,*]

[a] Department of Engineering and Chemical Sciences, Karlstad University, Karlstad, SE-651 88, Sweden
[b] Advanced Drug Delivery, Pharmaceutical Sciences, BioPharmaceuticals R&D, AstraZeneca, Mölndal, SE-431 83, Sweden

ARTICLE INFO

Keywords:
Peak integration
Co-eluting peaks
Chromatographic data systems
Impurity profiling
Analyst interaction

ABSTRACT

Peak integration is a major and often underestimated source of uncertainty in pharmaceutical LC–UV quality control (QC), particularly when minor impurity peaks appear as shoulders or rider peaks on the tails of overloaded active pharmaceutical ingredient (API) peaks. In routine QC, APIs are frequently injected at high concentrations to ensure sufficient sensitivity for impurity analysis, which can result in partial column overloading and pronounced peak tailing. Here, we systematically evaluated integration accuracy and analyst interaction for commonly used rule-based integration algorithms implemented in commercial chromatographic data systems (Agilent OpenLab and Waters Empower) and compared them with an in-house independent integration system (IIS). The assessment included synthetic chromatograms with known areas as well as experimental LC–UV data for metoprolol and six related impurities. For baseline-resolved symmetric peaks, relative integration errors remained within approximately ±1.5% across all systems. For partially overlapping symmetric peaks, integration errors depended on peak size, noise level, and the integration method applied. In several rider-peak scenarios, errors for the perpendicular drop method (PDM) exceeded 100%. Application of the exponential skim method (ESM) reduced errors considerably, typically to 10–30% and in some cases to below ±5%, although not consistently. In the selected complex cases, greater analyst interaction was required in the commercial systems, increasing the potential for user-dependent variability.

Overall, in the investigated cases, integration accuracy was strongly dependent on peak shape and overlap, with larger errors observed in asymmetric, shoulder, and rider-peak scenarios. These findings highlight the importance of integration-method selection and standardized integration practice in pharmaceutical LC–UV impurity analysis.

1. Introduction

Liquid chromatography with UV detection (LC–UV) remains a principal analytical technique for quantifying active pharmaceutical ingredients (APIs) and related impurities in small-molecule drug products. Although significant advances have been achieved in column technology, detector performance, and instrumentation, the final quantitative step, peak integration, continues to rely predominantly on geometric, rule-based algorithms developed during the early era of computerized chromatography [1–4]. Integration therefore remains a major source of analytical uncertainty [3,4].

Regulatory frameworks place strict requirements on the quantitative performance and control of analytical procedures used in pharmaceutical quality control (QC). ICH Q2(R2) defines validation expectations for analytical procedures, including accuracy, precision, linearity, lower range limits, and the reportable range [5], while ICH Q6A provides principles for scientifically justified specifications and acceptance criteria for assay and impurity determinations [6]. In addition, ICH Q3A(R2) and ICH Q3B(R2) define reporting, identification, and qualification thresholds for impurities in drug substances and degradation products in drug products, respectively [7,8]. Together, these requirements depend on reliable chromatographic peak-area measurement. In parallel, data-integrity guidance, including Parenteral Drug Association (PDA) Technical Report No. 80, emphasizes that chromatographic data processing, integration events, reprocessing, and audit trails should be controlled, traceable, and available for review [9].

* Corresponding author.
E-mail address: torgny.fornstedt@kau.se (T. Fornstedt).

https://doi.org/10.1016/j.jpba.2026.117740
Received 6 July 2026; Received in revised form 5 September 2026; Accepted 18 September 2026
Available online 21 September 2026
0731-7085/© 2026 The Author(s). Published by Elsevier B.V. This is an open access article under the CC BY license (http://creativecommons.org/licenses/by/4.0/).

The regulatory importance of chromatographic integration is further illustrated by recent FDA warning letters addressing inappropriate or insufficiently controlled reintegration practices [10,11]. Integration is therefore not merely a technical post-processing step, but a central component of pharmaceutical QC.

Commercial chromatographic data systems (CDSs) typically implement geometric integration strategies for partially resolved peaks, including the perpendicular drop method (PDM), valley-to-valley integration, and several skimming approaches such as tangential, exponential, and Gaussian skimming [1–3]. Of these, PDM and the skimming variants are most frequently applied in routine workflows. Previous investigations have demonstrated that significant quantification errors may arise for minor peaks under conditions of limited resolution or extreme peak-area ratios [12,13], and simulation studies have confirmed that peak overlap and asymmetry readily induce deviations from true areas [14,15]. In practice, integration accuracy depends on both the selected algorithm and user-defined parameters, including detection thresholds, slope sensitivity, peak width, baseline handling, and skimming ratios. Iterative parameter tuning guided by analyst judgment may improve local performance but can introduce subjectivity, potential inter-analyst variability, and compliance concerns if not transparently documented [2,9–11,16].

In LC–UV, challenges such as baseline variability, limited dynamic range, and asymmetric peak shapes persist. Experimentally validated, side-by-side comparisons of integration strategies across widely used commercial CDS platforms remain limited, despite their widespread use in pharmaceutical laboratories [2]; published work has largely addressed individual difficult cases, such as the quantification of rider peaks, rather than systematic cross-platform evaluation [17]. Recent developments in machine-learning-based peak detection and deconvolution have demonstrated promising performance for complex chromatographic data [18]. However, many such approaches target LC–MS applications, whereas fewer systematic evaluations have been conducted for UV-based chromatographic systems under regulated QC conditions.

The data-integrity and regulatory aspects of peak integration have also recently been reviewed for capillary electrophoresis [19]. Direct comparisons should, however, be drawn with caution, as electropherogram integration, particularly for capillary electrophoresis with sodium dodecyl sulfate of biomacromolecules, involves fundamentally different peak shapes and baseline characteristics than small-molecule LC–UV.

In a recently published simulation-based study of 40,000 symmetric Gaussian peak-overlap cases, systematic integration bias was demonstrated for commonly used rule-based methods under controlled conditions [20]. The analysis showed that integration errors increased rapidly with decreasing resolution, particularly affecting minor peaks in overlapping systems, and that algorithm-dependent differences arose even in ideal, noise-free geometries. These findings indicated that peak-overlap topology alone can introduce substantial quantitative bias. However, those simulations did not address overloaded, asymmetric API peaks or analyst interaction in commercial CDS workflows.

Building on that study [20], we extend the analysis beyond idealized symmetric Gaussian scenarios toward selected chromatographic conditions relevant to pharmaceutical QC. Using predominantly synthetic datasets spanning challenging peak geometries, including asymmetric overlap and overloaded API rider configurations, complemented by experimental small-molecule LC–UV data, we evaluate integration accuracy and analyst interaction across these selected conditions.

A demanding scenario in pharmaceutical QC arises when low-level organic impurities must be quantified in the presence of a heavily loaded and often asymmetric API peak. For new drug substances with a maximum daily dose of ≤ 2 g/day, ICH Q3A(R2) specifies a reporting threshold of 0.05% and a qualification threshold of 0.15% or 1.0 mg/day intake, whichever is lower [7]. For drug products, ICH Q3B(R2) specifies a qualification threshold of 1.0% or 50 μg total daily intake, whichever is lower, for a maximum daily dose of < 10 mg/day, whereas the qualification threshold is 0.15% for a maximum daily dose of > 2 g/day [8]. For early clinical development, higher qualification limits have been proposed under dose-limited conditions, including 0.7% for drug substances and 2.0% for drug products [21]. These impurity levels require analytical procedures with adequate accuracy and precision, in accordance with established validation practice [5,6,22–24]. The present study includes a 0.05% relative-area simulation, whereas several other selected synthetic and experimental cases involve higher impurity levels intended to investigate integration behavior under conditions relevant to impurity qualification and analytical method development.

The specific aim of this study was to systematically evaluate both the numerical accuracy and the degree of analyst interaction associated with commonly applied rule-based integration methods in pharmaceutical LC–UV QC. Synthetic chromatograms with known reference areas were generated to illustrate selected challenging peak geometries, including asymmetric overlap, shoulder formations, and rider peaks. These simulations were complemented by experimental LC–UV analyses of metoprolol and related impurities under API-overloaded conditions inspired by USP-relevant scenarios [25]. By comparing integration performance across commercial CDS platforms and using an in-house independent integration system (IIS), the study investigated integration accuracy and required analyst intervention across these selected chromatographic conditions, with particular emphasis on low-level impurity quantification, where reporting limits and acceptance margins are narrow.

2. Theory

2.1. Processing of chromatograms

A CDS is used to determine peak areas from measured chromatograms and is expected to provide accurate and reproducible results while minimizing manual user intervention. A classical analytical challenge in chromatographic data processing involves three distinct tasks: peak detection, that is, identifying the presence of chromatographic peaks; peak attribution (peak assignment), that is, assigning detected peaks to relative retention times and specific impurities; and peak-area integration, that is, defining peak boundaries and calculating the corresponding peak areas. A typical CDS workflow supports several of these tasks and commonly comprises the following computational steps: (1) noise reduction, (2) baseline estimation and correction, (3) peak detection, and (4) peak-area integration.

Commercial CDS platforms typically allow users to influence the underlying algorithms in three main ways: (1) selecting processing options, such as the integration algorithm; (2) tuning parameters, such as thresholds for peak detection; and (3) manual interaction, such as baseline adjustment. Most CDS platforms also provide a default “auto” mode for automated processing, with the option for manual refinement if the results are not satisfactory.

Common integration algorithms for overlapping peaks are shown in Fig. 1. Panel (A) depicts the PDM, while panels (B)–(D) show more advanced skim-based approaches. In the PDM, the individual peak areas are estimated by applying a vertical drop at the minimum between adjacent peaks and integrating the signal within the resulting boundaries (Fig. 1A). The PDM is a widely used rule-based approach and is commonly available in commercial CDS platforms.

In pharmaceutical QC, a challenging scenario can arise when low-level impurities elute as small “rider peaks” on the shoulder or tail of a dominant API peak. Because the main component may be present at a much higher concentration, the API peak can become overloaded and exhibit pronounced tailing on its descending side. In such cases, conventional methods such as the PDM can perform poorly, as the small impurity peak may be partly buried in the tail of the large API peak.

In these cases, special methods are sometimes used to estimate the areas of rider peaks, collectively referred to as skimming methods. These approaches attempt to separate the contribution of the small peaks from

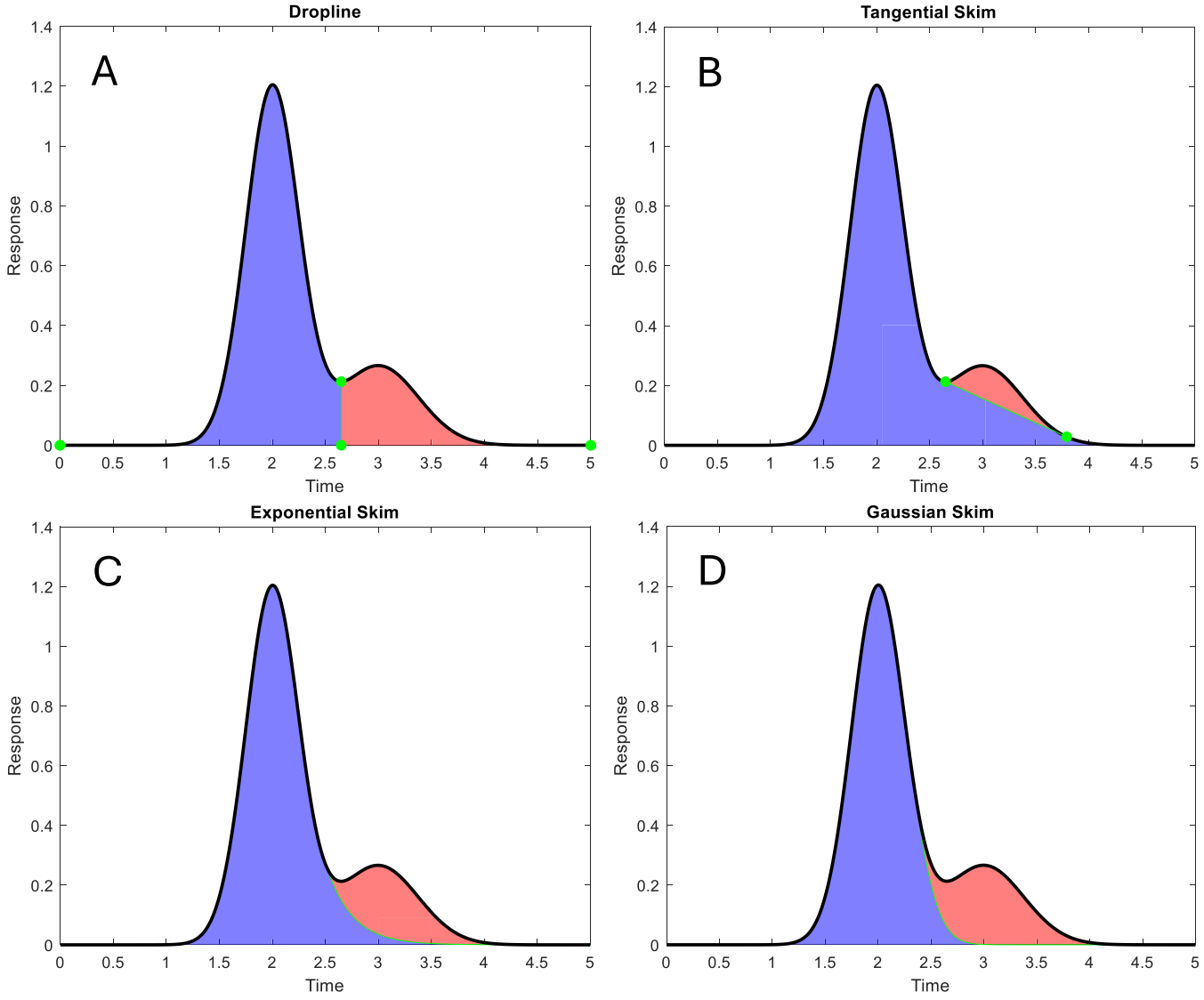

Fig. 1. Schematic representation of integration algorithms for overlapping peaks: (A) perpendicular drop method (PDM), (B) tangential skim method (TSM), (C) exponential skim method (ESM), and (D) Gaussian skim method (GSM).

that of the large peak and assign it an individual area. The area of the large peak is then obtained as the total response minus the sum of the rider peak areas. Three common skimming methods are shown in Fig. 1B–D. In the tangential skim method (TSM, Fig. 1B), a straight line is drawn from the valley between the large and the rider peaks to a tangential point on the observed total response curve. In the exponential skim method (ESM, Fig. 1C), an exponential decay function is fitted to the baseline after the rider peak and to part of the observed total response curve after the main peak apex but before the valley. The Gaussian skim method (GSM, Fig. 1D) is similar but instead fits a Gaussian peak function.

In this context, it is worth noting that skimming procedures, such as TSM, ESM, and GSM, are available in many commercial CDS platforms. However, vendor-specific differences in which skimming procedures are supported and how they are implemented are common.

To enable a fair assessment of different integration routines, an in-house routine termed IIS was developed. IIS applies predefined rules to ensure consistent and fully transparent algorithm execution across datasets, allowing detailed examination of each processing step. IIS is fully automated and does not contain any external user-tunable parameters, although it contains internal parameters that are adjusted based on the estimated noise level. It is implemented to provide controlled and transparent data processing and to enable an independent comparison of integration results. It is not intended to serve as a validated reference method.

Within IIS, the signal is segmented based on estimated noise variance, and baseline regions are automatically identified and corrected following Liu and Lin [26]. Extrema and shoulder points are detected without the use of derivatives after modified sinc filtering with automatic order selection [27]. Peak groups are subsequently integrated using PDM or, where appropriate, skimming methods.

2.2. Peak models

Synthetic chromatographic peaks were generated using a Gaussian model and the more flexible generalized error distribution II (GED II) model [28], allowing systematic variation of asymmetry and kurtosis. For the Gaussian model, the response is given by,

$$y(t) = \frac{a}{\sigma\sqrt{2\pi}} \exp\left(-\frac{(t-\mu)^2}{2\sigma^2} \right), \tag{1}$$

where t is time, $y(t)$ is response, a is peak area, μ is peak position, and σ is peak width.

For the GED II model, we have that,

$$y(t) = \frac{s_2(t)\cdot s_3(t)}{s_4\cdot s_5(t)},$$
$$s_1(t) = \sqrt{\sigma}\cdot\log\left(1+\frac{\tau}{\sigma}\left(t-\left(\sigma-\exp\left(\frac{\tau^2}{2}\right)\sigma+\mu\tau\right)\Big/\tau\right)\right),$$
$$s_2(t) = \exp\left(-\left|\frac{s_1(t)}{\tau}\right|^{\kappa}\cdot\frac{\sigma^{-\kappa/2}}{\kappa}\right), \quad (2)$$
$$s_3(t) = H\left(\mathrm{sgn}(\tau)\left(t-\mu+\frac{\sigma}{\tau}\exp\left(\frac{\tau^2}{2}\right)\right)\right)\cdot a\kappa^{-1/\kappa},$$
$$s_4 = 2\sqrt{\sigma}\cdot\Gamma(1+1/\kappa),$$
$$s_5(t) = \sqrt{\sigma}+\frac{\tau}{\sqrt{\sigma}}\left(t-\left(\sigma-\sigma\cdot\exp\left(\frac{\tau^2}{2}\right)+\mu\tau\right)\Big/\tau\right).$$

The parameters are defined as above, in addition τ is the peak-asymmetry parameter ($\tau < 0$ for fronting peaks and $\tau > 0$ for tailed peaks), κ is the peak kurtosis parameter governing the power of the peak front/tail decay, sgn is the sign function, H is the Heaviside function, and Γ is the gamma function.

For the overloaded API peak, the elution profiles were simulated using the equilibrium-dispersive model of chromatography with a nonlinear Langmuir adsorption isotherm [29]:

$$q(C) = \frac{aC}{1+bC}. \quad (3)$$

Here q and C are the stationary- and the mobile-phase concentrations, respectively, and a, b are adsorption-isotherm parameters.

3. Materials and methods

3.1. Chemicals and materials

The chemicals used for preparing mobile phases and solvents were gradient grade for liquid chromatography acetonitrile (MeCN) and liquid chromatography methanol (MeOH), both purchased from Sigma-Aldrich (Darmstadt, Germany). Phosphoric acid (85%) was obtained from Sigma-Aldrich, disodium hydrogen phosphate monohydrate (PhEur for analysis) from Supelco (Bellefonte, PA, USA), and water from a Milli-Q water purification system (Millipore Sigma, Burlington, MA, USA).

Metoprolol tartrate (CAS 56392–17–7, product PHR1076–1G), metoprolol impurity A (CAS 109632–08–8, product Y0000145), and metoprolol impurity E (CAS 163685–38–9, product PHR9101–100 mg) were purchased from Sigma-Aldrich. The metoprolol related impurities H9/64 (CAS 7695–63–8), H93/82 (CAS 62572–90–1), H177/19 (CAS 178968–86–0), and H158/16 (CAS 18966–02–4) were provided by AstraZeneca R&D (Gothenburg, Sweden) [30].

3.2. Instrumentation

All experiments were conducted on an Agilent 1200 LC–UV system (Agilent, Santa Clara, CA, USA), configured with a binary pump with degasser unit (SL G1312B), a column compartment (TCC SL G1316B), an autosampler (HiP-ALS G1367B), and a diode-array detector (DAD; SL G1315C). An Acquity UPLC HSS T3 C18 column (100 × 2.1 mm; 1.8 μm) from Waters Corporation (Milford, MA, USA) was used to analyze the samples. Chromatographic data were acquired as identical raw chromatograms for subsequent processing in the CDS platforms described in Section 3.3.1.

3.3. Procedures

3.3.1. Integration using CDS

Chromatographic data were processed using Agilent OpenLab CDS Data Analysis (Version 2.8) and Waters Empower Software (Version 3.8.0.2). Both systems were used in their standard configurations without modification of default algorithms beyond adjustments necessary to obtain acceptable peak delineation. No external scripts, custom macros, or third-party plugins were employed. OpenLab and Empower were selected for evaluation as examples of commonly used commercial CDS platforms in the pharmaceutical industry.

Initial processing of the synthetic chromatograms was performed before the simulation settings, peak positions, and true peak areas used for performance evaluation were disclosed. During subsequent evaluation, integration settings were explored with the aim of obtaining acceptable peak assignments while avoiding unnecessary user intervention. The reported commercial-CDS results should therefore be interpreted as analyst-optimized outcomes obtained during development and adjustment of integration settings, rather than as estimates of default, fully blinded, or routine sample-by-sample QC performance.

Fully automated integration using the CDS was initially tested. Because unacceptable integration results were observed for some chromatograms, manually adjusted integration settings were subsequently used for all chromatograms.

For each chromatogram, integration was performed using the simplest reproducible workflow available within each CDS. Given that multiple combinations of parameters can produce similar integrated areas, parameter settings were selected based on minimal manual intervention while achieving peak assignments in which the expected peaks were detected and the assigned boundaries were consistent with the intended integration algorithm. When several parameter combinations yielded comparable peak areas, the configuration requiring the fewest user actions was selected.

One analyst performed the CDS optimization. The study was not designed to quantify inter-analyst variability, and no statistical inference regarding analyst-to-analyst variability was made.

To enable systematic comparison of analyst interaction, the integration effort was quantified using two metrics: Clicks and User input.

Clicks were defined as discrete user-interface interactions required to configure and execute integration. These included activation of buttons, selection of tick boxes, opening and selecting options from drop-down menus, adjustment of sliders (e.g., skim ratio), and selection of fields enabling parameter modification. Each such interaction was counted as one click, irrespective of execution time.

User input was defined as explicit numerical parameter entry required before or during integration. This included the manual specification of slope sensitivity, fixed peak width, detection thresholds, skim ratio (if adjusted numerically or via slider), minimum peak height, and similar quantitative settings. Each distinct numerical parameter adjustment was counted as one user input, regardless of the magnitude of the value entered.

Clicks and numerical parameter inputs were used only as descriptive measures of analyst interaction within the evaluated workflows. They should not be interpreted as direct measures of peak difficulty, analytical complexity, user effort, processing time, or quantitative differences in platform performance. These metrics can be influenced by software configuration, default settings, workflow design, and analyst familiarity.

Importantly, the counting of clicks and user inputs deliberately excluded all steps related to data importing, sample loading, chromatogram selection, data processing unrelated to integration (e.g., smoothing), report generation, and viewing or exporting results. Only interactions directly required to obtain an annotated peak area for the chromatographic peaks under investigation were included. The purpose of this definition was to isolate the user interaction specifically associated with peak integration rather than general data handling within the CDS environment.

Detailed descriptions of the specific actions performed for each chromatogram and integration method are provided in the Supplementary Material (Tables S5–S7 and Figs. S2 and S3).

3.3.2. Experimental

The samples were prepared as follows. A metoprolol tartrate stock solution of 5 mg/mL was prepared by dissolving metoprolol tartrate in MeCN and subsequently diluting with water to obtain a 50:50 (v/v) water/MeCN solution. Impurity stock solutions were prepared at 1 mg/mL for Impurity A, Impurity E, H93/82, and H9/64, and at 2 mg/mL for H177/19, by dissolution in MeCN followed by dilution with water to obtain 50:50 (v/v) water/MeCN solutions. H158/16 was initially dissolved in MeOH and subsequently diluted with water to obtain a 90:10 (v/v) water/MeOH solution. All impurity stock solutions were then further diluted to 0.1 mg/mL using 90:10 (v/v) water/MeCN as the dilution medium before preparation of the mixed solutions.

The mixed solutions for injection, with and without metoprolol, were prepared to final concentrations of 1 mg/mL metoprolol tartrate and 0.01 mg/mL of each individual impurity. The solutions were prepared volumetrically using 90:10 (v/v) water/MeCN as the dilution medium. The mobile phases were phosphate buffer at pH 3 in water (I = 0.05 M) (mobile phase A) and 100% MeCN (mobile phase B).

All chromatograms were recorded at a wavelength of 225 nm with a 4-nm bandwidth and a reference wavelength of 360 nm with a 50-nm bandwidth, at a sampling rate of 40 Hz. Separations were conducted using an injection volume of 4 µL, with the column compartment maintained at 45 °C. Gradient separations were performed at a flow rate of 0.4 mL/min using a gradient from 15% to 65% mobile phase B over 11 min, followed by re-equilibration at 15% mobile phase B for 5 min. The total run time was 16 min.

The experimental separation was used as a controlled chromatographic model system for evaluating peak-integration performance and was not intended as a validated quantitative assay.

3.4. Calculations

In Fig. 2A, synthetic chromatograms were generated using the Gaussian model, Eq. (1), to illustrate the elution of the API and impurity peaks. The API peak ($\mu = 6.85$ min, $\sigma = 0.0143$ min) had an area of 1240 mAU·s, while the impurity peak ($\sigma = 0.934$ s) had an area of 0.6203 mAU·s (0.05% relative area). The impurity retention time (6.920–7.01 min) approached the shoulder limit, with resolution at 10% peak height ranging from 2.5 to 1.12.

For the chromatograms presented in Fig. 2B, the main peak elution profiles were simulated using the equilibrium-dispersive model solved using the Rouchon finite-differences algorithm [29] (see Table S1 for system and column properties). The simulated chromatographic system was scaled to a column internal diameter of 2.1 mm, a flow rate of 0.255 mL/min, and an injection volume of 12.9 µL while maintaining the same linear velocity and column loading. The column efficiency (16,000 theoretical plates), porosity (0.624), and phase ratio (0.602) were retained (Table S1). This rescaling does not alter the simulated chromatogram. The area of the API peak was 15,237 mAU·s and the asymmetry factor, A_{sf}, calculated at 10% peak height was 7.5. The impurity peak was simulated using the Gaussian model, Eq. (1), with $\sigma = 1.250$ s and an area of 7.622 mAU·s (0.05%). The impurity retention time (5.78–5.87 min) approached the shoulder limit, with resolution at 10% peak height ranging from 2.5 to 2.06.

For the Gaussian model, Eq. (1), two synthetic chromatograms were generated to illustrate binary peak overlap (Fig. 3B). The specific peak parameters are provided in the Supplementary Material (Table S2).

For the GED II model, see Eq. (2), five synthetic chromatograms (Fig. 3A, C-F) were generated with added noise characterized by color c_{noise} and standard deviation σ_{noise}. Kurtosis, κ, was set to 2. The complete set of peak and noise parameters is provided in the Supplementary Material (Table S3).

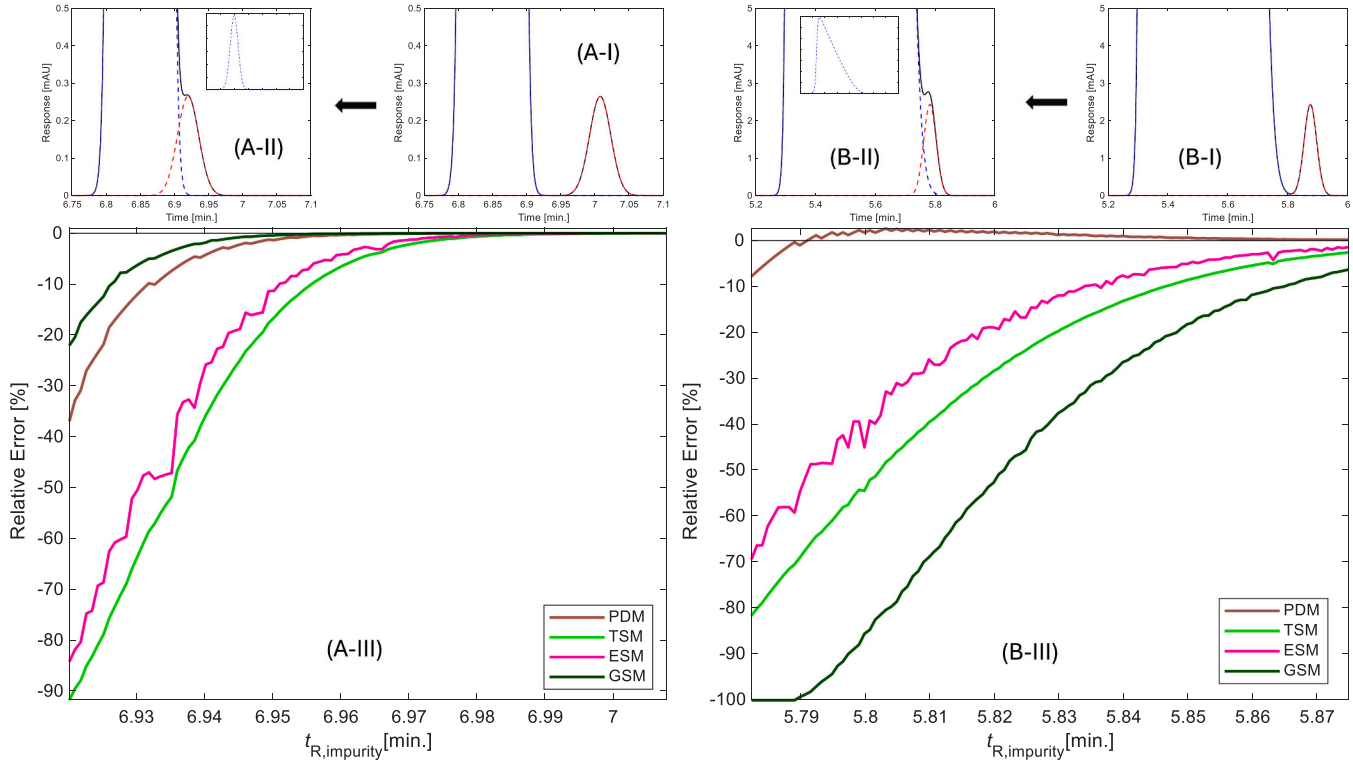

Fig. 2. Simulated integration of a minor impurity peak with a relative area of 0.05% in the presence of a dominant API peak. (A) System with Gaussian API and impurity peaks. Peak overlap increases from baseline-separated peaks (A–I) to an almost fully merged system (A–II); the inset in (A–II) shows a zoomed-out view of the dominant API peak. (A–III) Relative impurity-area error as a function of overlap using the perpendicular drop method (PDM, brown), tangential skim method (TSM, light green), exponential skim method (ESM, magenta), and Gaussian skim method (GSM, dark green). (B) Corresponding simulations with an overloaded asymmetric API peak and the same 0.05% relative impurity area. The inset in (B–II) shows a zoomed-out view of the dominant API peak.

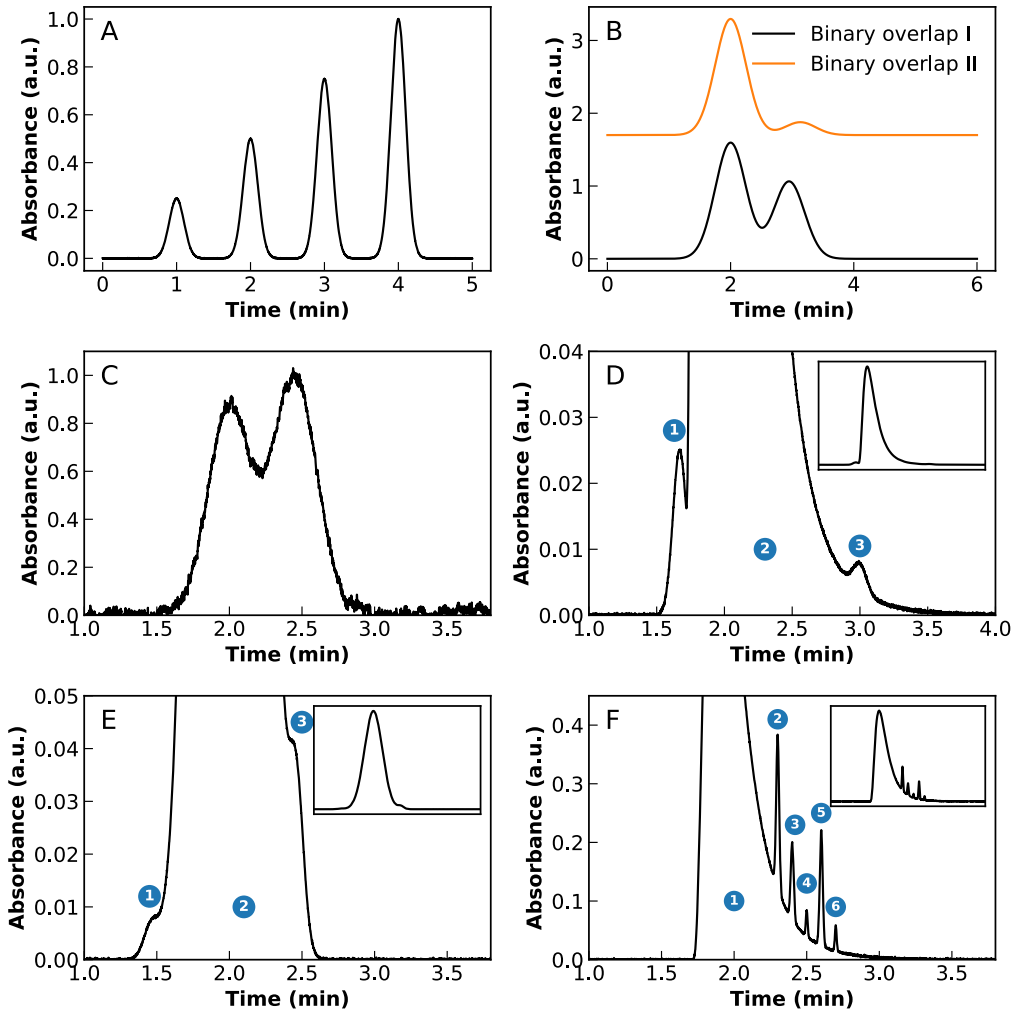

Fig. 3. Synthetic chromatograms used to evaluate peak integration algorithms across selected peak geometries and chromatographic conditions: (A) four symmetric, baseline-resolved peaks; (B) two symmetric, partially overlapping peaks differing in relative peak area; (C) partially overlapping symmetric peaks in the presence of elevated pink baseline noise; (D) asymmetric overlap with minor peaks eluting on the leading edge and tail of a dominant peak; (E) shoulder peaks adjacent to a dominant component; and (F) multiple rider peaks eluting on the tail of an asymmetric dominant peak. Insets show enlarged views of selected regions.

In all simulations, the resulting data points corresponded to a sampling frequency of 20 Hz. For synthetic chromatograms, relative integration error was calculated as

$$\text{Error}(\%) = 100\frac{A_{\text{int}} - A_{\text{Ref}}}{A_{\text{Ref}}} \quad (4)$$

where A_{int} is the integrated peak area and A_{Ref} is the known input peak area used to generate the chromatogram. For the experimental metoprolol chromatograms, the corresponding impurity peak area in the impurity-only chromatogram was used as a comparative reference (A_{Ref}), rather than as an absolute ground-truth value, and A_{int} was the area obtained for the same impurity in the metoprolol-containing chromatogram. In an additional normalized analysis, all impurity peak areas were normalized to the area of the baseline-resolved Peak 2 within the corresponding chromatogram. The normalized relative areas obtained from the impurity-only chromatogram were then compared with the corresponding normalized relative areas in the metoprolol-containing chromatogram. The resulting normalized relative integration errors are reported in Table S8.

4. Results and discussion

Previous simulations of symmetric, equal-width Gaussian peaks [20] indicated that the PDM often yielded the lowest relative error under those specific, ideal conditions. The present study extends this analysis to selected additional peak geometries in which the assumptions of symmetry and equal peak width are relaxed, including asymmetric overlap and overloaded API rider configurations.

Accordingly, before addressing the selected cases in Sections 4.2 and 4.3, Section 4.1 examines how integration behavior changes when the assumptions of peak symmetry and equal width are progressively relaxed.

Sections 4.1 and 4.2 are based on simulated chromatograms, whereas Section 4.3 is based on experimental data. The simulated chromatograms contain predefined peak positions and input peak areas, providing exact ground truth for post hoc assessment of integration accuracy. These true values were not disclosed during the initial processing of the synthetic chromatograms. In contrast, the experimental chromatograms do not provide an equivalent absolute ground truth; the impurity-only chromatograms are used as comparative references and may themselves be affected by normal run-to-run analytical variability. Simulations therefore provide a controlled framework for quantitative assessment of integration performance, while the experimental chromatograms complement this analysis by incorporating realistic noise, peak-shape, and co-elution effects.

4.1. From ideal peak overlap to overloaded API overlap

In Fig. 2, we illustrate the transition from ideal symmetric Gaussian overlap (Fig. 2A) to a selected simulated case involving an overloaded and asymmetric API peak (Fig. 2B). In both cases, the relative area of the impurity is 0.05%. In the symmetric case (Fig. 2A), both the API peak and the following impurity peak are Gaussian, although the former is much broader. Under these specific conditions, all evaluated methods underestimate the impurity peak area. The GSM and PDM show relatively smaller errors than the TSM and ESM; however, both still result in underestimation of the impurity peak area.

When the API peak is both broader and asymmetric (Fig. 2B), its tail no longer follows Gaussian decay, which violates the underlying assumption of the GSM. In this simulated case, the PDM becomes sensitive to the sloping API tail and tends to assign part of this signal to the impurity, resulting in overestimation for most of the investigated resolutions. Under these conditions, the exponential skim method (ESM) gives the smallest error among the skim methods, whereas the GSM gives the largest errors.

It should be noted that the practical consequences of overestimation and underestimation are not equivalent. From a patient-safety and impurity-control perspective, the positive bias produced by the PDM may be considered conservative because it reduces the risk of an impurity being overlooked or reported below its true level. Conversely, underestimation may be more critical because it can result in an impurity being reported below its actual level and, depending on the applicable threshold or specification, may mask a relevant exceedance. From a manufacturing perspective, however, overestimation may increase the risk of unnecessary investigations or rejection of batches that actually meet specifications. Thus, the numerical magnitude of an integration error should be distinguished from the practical consequences associated with the direction of the bias.

These simulations show that the magnitude and direction of integration bias depend strongly on peak geometry. For the asymmetric, overloaded API configuration investigated here, PDM showed the smallest absolute errors over most of the investigated range, while ESM showed the smallest errors among the skim methods. In the following sections, we examine selected additional peak-shape scenarios to further assess integration performance under different chromatographic conditions.

Increasing the relative impurity area to 0.25% for the symmetric case and 0.35% for the asymmetric overloaded case yielded trends similar to those observed at the 0.05% impurity level (Fig. S1). The relative performance of the evaluated methods was broadly similar, while the magnitude of the relative errors decreased, resulting in more accurate impurity-area estimates.

4.2. Synthetic studies

Integration performance was initially assessed using synthetic chromatograms comprising fully baseline-resolved symmetric Gaussian peaks (Fig. 3A), partially overlapping symmetric peaks (Fig. 3B), and partially overlapping peaks evaluated under elevated pink baseline-noise conditions (Fig. 3C). The corresponding results are summarized in Table 1, with additional details provided in Supplementary Tables S4 and S5.

The integration algorithms were then evaluated using selected synthetic chromatograms illustrating additional challenging peak geometries (Fig. 3D–F). These datasets are intended as illustrative examples rather than as a comprehensive or systematic description of chromatographic complexity. They include asymmetric overlap, shoulder formation, and rider peaks eluting on the tail of a dominant component. Because several factors, including peak-area ratio, resolution, asymmetry, tailing, and noise, vary among these cases, the results should be interpreted in relation to the specific peak geometries and conditions investigated rather than as demonstrating a general monotonic relationship between chromatographic complexity and integration performance. Integration accuracy and user interaction metrics for these datasets are summarized in Table 2, with additional details provided in Supplementary Tables S4 and S6.

Table 1
Relative integration errors and user interaction for simple synthetic chromatograms analyzed using IIS (see Section 2.1), Agilent OpenLab, and Waters Empower. Integration accuracy is reported as relative error (%) with respect to the known input peak areas. User interaction is reported as the total number of mouse clicks and numerical parameter inputs required to obtain final peak areas. Detailed workflow descriptions are provided in the Supplementary Material (Table S5). Abbreviations: IIS, independent integration system; PDM, perpendicular drop method; GSM, Gaussian skim method.

		IIS		OpenLab		Empower	
	Peak	PDM	GSM	PDM	GSM	PDM	GSM
Reference (Fig. 3A)	1	–0.7%	-	-0.9%	-	1.4%	-
	2	–0.2%	-	–0.1%	-	0.7%	-
	3	0.0%	-	–0.1%	-	0.6%	-
	4	–0.2%	-	0.1%	-	0.5%	-
Clicks		N/A	N/A	3	-	3	-
User inputs		N/A	N/A	0	-	1	-
Binary overlap I (Fig. 3B)	1	0.7%	3.5%	0.6%	3.7%	2.1%	9.5%
	2	–1.0%	–5.2%	–0.9%	–5.5%	0.9%	–10.2%
Clicks		N/A	N/A	4	6	3	5
User inputs		N/A	N/A	2	3	1	1
Binary overlap II (Fig. 3B)	1	0.3%	0.1%	0.3%	0.9%	1.4%	1.7%
	2	–3.1%	–0.8%	–3.0%	–8.2%	5.2%	1.6%
Clicks		N/A	N/A	4	6	1	4
User inputs		N/A	N/A	2	3	0	1
Binary overlap with noise (Fig. 3C)	1	–5.1%	-	5.7%	-	5.8%	-
	2	2.2%	-	5.6%	-	6.4%	-
Clicks		N/A	N/A	4	-	1	-
User inputs		N/A	N/A	2	-	0	-

From an analytical chemistry perspective, chromatographic analysis involves several distinct tasks: peak detection, peak attribution (peak assignment), and peak-area integration. Peak-area integration is the primary focus of the present work and is discussed in detail below. However, the chromatograms shown in Fig. 3D–F may also illustrate challenges related to peak detection and peak attribution. In particular, the shoulder peaks in Fig. 3E illustrate that the primary challenge may be determining whether a separate peak is present and should be assigned before its integration boundaries can be defined.

Details of the peak simulations are presented in Supplementary Tables S2 and S3. The chromatographic properties of the separations shown in Fig. 3, including peak-area ratios, resolution, asymmetry, and tailing factors, are presented in Table S4.

4.2.1. Symmetric resolved peaks as reference

The first synthetic dataset consists of four fully baseline-resolved symmetric Gaussian peaks (Fig. 3A). Under these ideal conditions, all evaluated approaches, Agilent OpenLab, Waters Empower, and IIS, showed close agreement with the known peak areas, with relative integration errors within approximately ±1.5% for all peaks (Table 1). Because no peak overlap or baseline distortion was present, all peaks were readily detected and integrated by the evaluated systems. Only limited adjustment of processing parameters was required in the commercial CDS platforms, and no baseline adjustment, skimming, or manual integration was necessary.

4.2.2. Symmetric overlapping peaks

To further challenge the integration algorithms, a second synthetic dataset consisting of two partially overlapping symmetric peaks was analyzed (Fig. 3B). Two separation conditions were investigated. In the first, the area of the second peak was two-thirds that of the first peak,

Table 2
Relative integration errors and required user interaction for selected synthetic chromatograms with asymmetric, shoulder, and rider-peak configurations analyzed using IIS, Agilent OpenLab, and Waters Empower. Integration accuracy is reported as relative error (%) with respect to the known input peak areas. User interaction is reported as the total number of mouse clicks and numerical parameter inputs required to obtain final peak areas. Detailed workflow descriptions are provided in the Supplementary Material (Table S6). Abbreviations: IIS, independent integration system; PDM, perpendicular drop method; ESM, exponential skim method.

		IIS		OpenLab		Empower	
	Peak	PDM	ESM	PDM	ESM	PDM	ESM
Tail overlap	1	–25.9%	–50.6%	–15.6%	–18.3%	–14.3%	–15.1%
(Fig. 3D)	2	–0.7%	–0.3%	–0.2%	0.2%	–0.2%	0.0%
	3	106.9%	–16.4%	255.9%	11.2%	239.8%	30.4%
Clicks		N/A	N/A	4	6	1	6
User inputs		N/A	N/A	2	3	0	0
Shoulders	1	8.8%	–66.4%	29.0%	–17.7%	3.5%	1.0%
(Fig. 3E)	2	–0.1%	0.8%	–0.3%	0.4%	–0.2%	0.6%
	3	8.5%	–66.1%	34.4%	–25.9%	28.5%	–56.7%
Clicks		N/A	N/A	2	3	10	14
User inputs		N/A	N/A	0	1	2	5
Tail riders	1	–8.7%	–1.5%	–8.3%	0.0%	–8.7%	–0.7%
(Fig. 3F)	2	160.2%	–2.6%	171.8%	–0.7%	157.5%	–2.0%
	3	193.5%	–1.0%	209.7%	–0.8%	178.9%	–1.8%
	4	392.6%	0.3%	474.2%	15.3%	368.9%	10.9%
	5	39.7%	–0.1%	53.7%	4.3%	35.5%	–33.4%
	6	161.3%	17.1%	702.5%	64.4%	67.7%	11.5%
Clicks		N/A	N/A	7	9	4	13
User inputs		N/A	N/A	2	3	1	4

with a resolution of 0.95; in the second, the area of the second peak was one-ninth that of the first peak, with a resolution of 1.13. Additional details of the peak simulations and chromatographic properties are provided in Tables S2 and S4. Compared with the fully resolved reference chromatogram, partial overlap makes the placement of peak boundaries more ambiguous.

For these datasets, PDM generally produced relatively small integration errors across the evaluated systems. For the larger peak, the relative errors ranged from 0.3% to 2.1%, whereas errors for the smaller peak ranged from −3.1–5.2% (Table 1). The effect of applying GSM depended on the degree of overlap, peak identity, and software system, and no consistent improvement over PDM was observed.

The partially overlapping peaks also resulted in differences in the amount and type of analyst interaction required by the commercial CDS platforms. Depending on the software and integration method, the required actions included adjustment of slope sensitivity and peak-width settings, specification of minimum-area thresholds, and selection or adjustment of skimming parameters. The extent of these interactions varied among the evaluated workflows (Table 1 and Table S5).

The reported number of user actions should be interpreted with caution, as this metric is influenced by software configuration, default settings, workflow design, and analyst familiarity with the platform. Consequently, it should not be considered a direct measure of analytical complexity, user effort, processing time, or quantitative platform performance. Rather, it provides a descriptive measure of analyst interaction within the evaluated workflows.

To assess the effect of signal variability, partially overlapping symmetric peaks with a resolution of 0.75 were also evaluated in the presence of elevated pink baseline noise (Fig. 3C). Pink noise (flicker noise) was selected because chromatographic baseline noise can exhibit temporal correlation and 1/f-type behavior rather than independent fluctuations [31]. The added noise was therefore intended to represent temporally correlated baseline fluctuations and to provide a more challenging integration case. Peak geometry remained symmetric, but peak detection and boundary assignment were affected by the increased signal noise.

Relative integration errors were within approximately ±6.5% for the evaluated PDM approaches (Table 1). The commercial CDS workflows differed in their response to the added noise. OpenLab required adjustment of slope sensitivity and peak-width parameters, whereas the evaluated Empower workflow required no numerical parameter input for this chromatogram (Table S5). Detailed descriptions of the individual user actions are provided in Supplementary Table S5.

Taken together, the results in Fig. 3A–C show that relatively small integration errors can be obtained for baseline-resolved and moderately overlapping symmetric peaks using PDM, although the magnitude and direction of the errors depend on peak overlap, noise, integration method, and software implementation. The amount of analyst interaction also varied among the evaluated commercial CDS workflows. These interaction metrics are descriptive and should not be interpreted as direct measures of chromatographic difficulty or comparative platform performance.

4.2.3. Asymmetric overlap with tailing

The first selected case involves asymmetric overlap, with minor peaks eluting on the leading edge (peak 1) and on the tail (peak 3) of a larger peak (peak 2) (Fig. 3D). This configuration illustrates how peak asymmetry and partial co-elution can complicate peak detection, peak attribution, and the definition of integration boundaries. Peaks 1 and 3 have peak-area ratios, defined as the area of each peak relative to the total peak area, of 0.99% and 0.16%, respectively (Table S4). The 0.16% ratio for peak 3 is close in magnitude to the 0.15% qualification threshold for new drug substances discussed in the Introduction.

The PDM produced substantial integration errors for the smallest peak (peak 3) in all evaluated systems, with relative errors exceeding 100% in each case (Table 2). In contrast, the dominant peak (peak 2) was integrated with comparatively small error. The area assigned to the minor peaks was more sensitive to the placement of integration boundaries, resulting in substantial overestimation or underestimation.

Application of the ESM substantially reduced the magnitude of the error for peak 3, from 106.9% to 255.9% with PDM to approximately 11–30% in absolute magnitude, depending on the evaluated system (Table 2). However, ESM did not consistently improve the integration of all peaks; for peak 1, the magnitude of the negative error increased in each system. Thus, no evaluated system or integration method showed uniformly superior accuracy across all peaks in this selected chromatogram.

From a workflow perspective, this chromatogram required different levels and types of analyst interaction in the two commercial CDS platforms. OpenLab required numerical adjustment of integration parameters, with two user inputs for PDM and three for ESM. Empower required no numerical parameter inputs for this chromatogram, although additional workflow actions were required when ESM was applied. The observed click counts and parameter inputs therefore

reflect the specific software configurations and workflows used and should be interpreted as descriptive measures of analyst interaction rather than as direct measures of chromatographic difficulty or platform performance.

4.2.4. Asymmetric overlap with shoulder peaks

The second selected case consists of shoulder peaks partially resolved from a dominant peak (Fig. 3E). The main component is peak 2, while peak 1 appears as a small leading shoulder and peak 3 as a trailing shoulder. The relative peak-area ratios of peaks 1 and 3 are 0.20% and 0.99%, respectively (Table S4). The resolution between peaks 1 and 2 is 1.35, whereas that between peaks 2 and 3 is 1.15. Because of the low relative areas of the shoulder peaks, no clear valley is present. In this configuration, the primary analytical challenge may therefore be determining whether a separate peak is present and should be assigned before its integration boundaries can be defined. Peak detection and attribution can consequently become sensitive to detection thresholds and algorithmic assumptions.

Using PDM, appreciable relative errors were observed for the shoulder peaks, although their magnitude varied among the evaluated systems. For peak 1, the relative errors ranged from 3.5% to 29.0%, whereas for peak 3 they ranged from 8.5% to 34.4% (Table 2). The absence of a well-defined valley therefore affected the assignment of integration boundaries for these low-level shoulder peaks.

Application of ESM substantially altered the error pattern but did not provide a consistent improvement. For peak 1, relative errors ranged from 1.0% to −66.4%, whereas for peak 3 all evaluated ESM implementations underestimated the peak area, with errors ranging from −25.9% to −66.1% (Table 2). Thus, skimming improved some individual results while substantially increasing the magnitude of the error in others.

These results indicate that, for this selected shoulder configuration, skimming-based approaches do not provide a generally accurate solution and may introduce integration-method-dependent bias. No individual software system or integration method showed uniformly superior accuracy across both shoulder peaks.

The commercial CDS workflows also differed markedly in the amount and type of analyst interaction required for this chromatogram. OpenLab required two clicks and no numerical parameter inputs with PDM, and three clicks and one numerical input with ESM. Empower required ten clicks and two numerical inputs with PDM, increasing to fourteen clicks and five numerical inputs with ESM (Table 2). The required actions included explicit shoulder detection, adjustment of detection-related parameters, configuration of skimming settings, and, in some workflows, baseline or dropline adjustments (Table S6). These differences should be regarded as descriptive characteristics of the evaluated workflows and not as direct measures of chromatographic difficulty, user effort, or comparative platform performance.

4.2.5. Rider peaks on the tail of a dominant peak

The largest integration errors among the selected synthetic cases were observed for the chromatogram containing multiple rider peaks (peaks 2–6) eluting on the tail of a dominant asymmetric peak (peak 1) (Fig. 3F). This configuration illustrates a rider-peak situation relevant to impurity analysis, in which several minor peaks are superimposed on a sloping dominant-peak tail. Several rider peaks are present at low relative abundance; in particular, peaks 4 and 6 each have a peak-area ratio of 0.20% relative to the total peak area (Table S4).

For this dataset, PDM produced extremely large integration errors for several rider peaks in all evaluated systems. Relative errors exceeded + 100% for several peaks and exceeded + 300% in multiple cases (Table 2). The most extreme value was observed for peak 6 in OpenLab, with a relative error of + 702.5%. These extreme deviations illustrate the difficulty of assigning the contribution of small rider peaks when they are superimposed on the sloping tail of a dominant peak.

Application of ESM substantially reduced the magnitude of the integration errors for several rider peaks. For peaks 2 and 3, the relative errors were within approximately ±3% in all evaluated systems, and similarly small errors were obtained for several other individual peaks (Table 2). However, the improvement was not consistent across the complete chromatogram. Larger deviations remained for some peaks, including peak 4 in OpenLab and Empower, peak 5 in Empower, and peak 6 in all three evaluated systems. Thus, although ESM substantially improved integration for several rider peaks in this selected configuration, it did not provide uniformly accurate results across all peaks and systems.

The commercial CDS workflows required multiple user actions to obtain the reported analyst-optimized results. For OpenLab, PDM and ESM required seven and nine clicks, respectively, with two and three numerical parameter inputs. For Empower, the corresponding values were four and thirteen clicks and one and four numerical parameter inputs (Table 2). The required actions included adjustment of peak-width and detection-related parameters, configuration of skimming settings, and, depending on the workflow, changes to baseline-processing options (Table S6). As in the preceding cases, these counts should be interpreted as descriptive measures of analyst interaction within the specific workflows rather than as direct measures of chromatographic difficulty, user effort, processing time, or comparative platform performance.

Across the selected chromatograms in Fig. 3D–F, the largest integration errors were generally associated with minor peaks in asymmetric, shoulder, and rider-peak configurations. PDM produced particularly large errors for several minor peaks, whereas ESM reduced the error substantially in some configurations but did not provide uniformly accurate results. The magnitude and direction of the integration error therefore depended on the specific peak geometry, integration method, and software implementation.

The amount and type of analyst interaction also varied among the evaluated commercial CDS workflows and chromatograms. These observations indicate that, for the selected cases investigated here, integration outcomes depend not only on the integration algorithm but also on the processing settings and workflow used to obtain the final peak areas. The following section examines related integration behavior using experimental chromatograms.

4.3. Experimental data

The final evaluation was performed using experimental LC–UV chromatograms of metoprolol and related impurities in a selected small-molecule model system inspired by a USP-relevant metoprolol impurity scenario [25]. Fig. 4A shows a mixture of six structurally relevant metoprolol impurities analyzed under gradient elution conditions. Fig. 4B shows the same impurity mixture in the presence of metoprolol at a substantially higher concentration, resulting in partial co-elution of impurities 3–5 on the descending tail of the dominant API peak.

A simplified small-molecule model system was intentionally selected to complement the simulation studies with experimental noise, peak shapes, and co-elution effects. The chromatographic method was designed to highlight selected integration-related challenges rather than to represent an optimized or validated QC method. Because the expected impurities had been injected separately, the analyst performing the CDS processing had prior knowledge of their presence, which may have facilitated peak detection and attribution, particularly for low-intensity or partially resolved peaks. The present study therefore focuses primarily on peak-area integration rather than on the detection of unidentified peaks. This distinction limits the generalizability of the findings to applications in which peak detection itself represents the primary analytical challenge.

For the non-normalized analysis, relative integration errors were calculated by comparing impurity peak areas obtained from the metoprolol-containing chromatogram (Fig. 4B) with the corresponding areas in the impurity-only chromatogram (Fig. 4A), which were used as

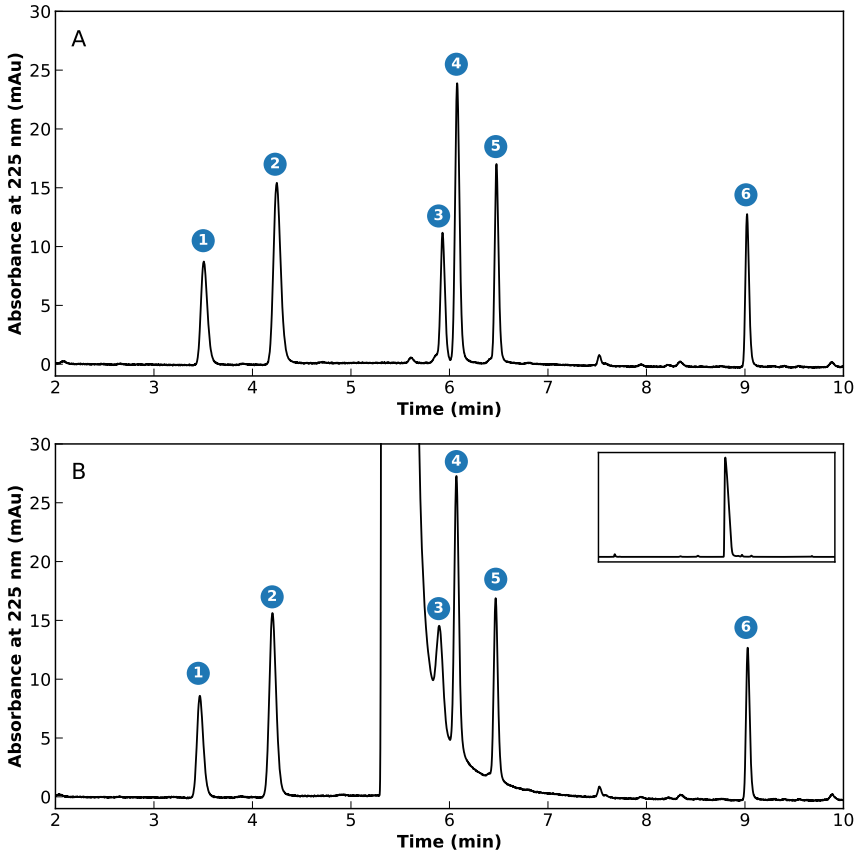

Fig. 4. Experimental LC–UV chromatograms used to evaluate peak integration: (A) mixture of six impurities related to metoprolol; (B) the same impurity mixture in the presence of metoprolol at a substantially higher concentration, resulting in partial co-elution of impurities 3–5 on the descending metoprolol signal. The inset in (B) shows a zoomed-out view of the dominant metoprolol peak.

comparative reference values rather than as absolute ground truth. The two samples were prepared from the same impurity mixture, with equal dilution applied in both cases. Nevertheless, ordinary run-to-run analytical variability may contribute to differences in absolute peak areas between chromatograms. Because replicate measurements were not used to quantify this variability, the experimental integration errors should be interpreted more cautiously than those obtained from the synthetic chromatograms, for which the true input areas are known exactly.

The local background in Fig. 4B is elevated and sloping for impurities eluting on the descending metoprolol signal, particularly peaks 3 and 4. Relative to their local background, the apparent heights of peaks 3–5 are similar to those observed in Fig. 4A, and the total UV response at the maxima of these impurity peaks remains below approximately 30 mAU. A contribution from detector non-linearity cannot, however, be completely excluded under these conditions. The elevated and sloping metoprolol background is therefore considered primarily relevant to baseline assignment and integration of the impurity peaks, while detector non-linearity remains a possible additional source of uncertainty.

Using PDM, substantial positive integration errors were observed for the co-eluting impurities 3–5 in all evaluated systems (Table 3). For the two commercial CDS platforms, PDM errors for these peaks ranged from + 26.1% to + 175.1%, with several values exceeding + 50%. In contrast, the non-overlapping peaks 1, 2, and 6 showed comparatively small PDM errors. This pattern is consistent with the synthetic rider-peak case in Section 4.2.5, in which assignment of minor-peak areas

Table 3
Relative integration errors and required user interaction for the experimental chromatograms analyzed using IIS, Agilent OpenLab, and Waters Empower. Integration accuracy is reported as relative error (%) with respect to the comparative reference areas obtained from the impurity-only chromatogram (Fig. 4A). User interaction is summarized as the total number of mouse clicks and numerical parameter inputs required to obtain final integrated peak areas. Detailed descriptions of the individual user actions and workflow steps are provided in the Supplementary Material (Table S7). Abbreviations: IIS, independent integration system; PDM, perpendicular drop method; ESM, exponential skim method.

		IIS		OpenLab		Empower	
	Peak	PDM	ESM	PDM	ESM	PDM	ESM
Metoprolol	1	–3.9%	N/A	–0.6%	N/A	1.5%	N/A
(Fig. 4B)	2	–4.5%	N/A	–2.2%	N/A	1.5%	N/A
	3	159.9%	–20.5%	173.8%	–9.3%	175.1%	–23.1%
	4	57.5%	–5.7%	70.8%	1.8%	81.7%	–38.8%
	5	153.5%	–3.7%	26.1%	–4.3%	71.0%	–4.2%
	6	–1.6%	N/A	1.1%	N/A	1.8%	N/A
Clicks		N/A	N/A	5	11	6	12
User inputs		N/A	N/A	0	2	2	4

was strongly affected by the presence of a sloping dominant-peak tail.

Application of ESM substantially reduced the magnitude of the integration errors for several of the co-eluting impurities. However, the improvement was not uniform across peaks and systems. For the commercial CDS platforms, ESM errors for impurities 3–5 ranged from −38.8% to + 1.8%, with the largest absolute deviation observed for peak 4 in Empower (Table 3). Thus, skimming considerably improved several individual integration results but did not eliminate integration bias for all peaks in this experimental chromatogram.

The IIS results further illustrate that automated processing without external user-tunable parameters does not by itself eliminate integration error. IIS produced substantial errors for the co-eluting impurities when PDM was applied, whereas ESM markedly reduced the errors but did not eliminate them in all cases (Table 3). These results are interpreted as an independent comparison of integration behavior rather than as performance against a validated reference method.

The commercial CDS results represent analyst-optimized outcomes obtained during development and adjustment of the integration settings. For OpenLab, PDM and ESM required five and eleven clicks, respectively, with zero and two numerical parameter inputs. For Empower, the corresponding values were six and twelve clicks and two and four numerical parameter inputs (Table 3). The workflow involved adjustment of integration ranges, peak-detection and peak-width parameters, skimming settings, and, depending on the software, baseline-processing options (Table S7). These interaction counts are descriptive measures of the specific workflows evaluated and should not be interpreted as direct measures of peak difficulty, user effort, processing time, or quantitative platform performance. Nor should these optimization workflows be regarded as estimates of routine sample-by-sample QC processing.

To reduce the influence of run-to-run variability, an additional analysis was performed in which peak areas were normalized to Peak 2, which was baseline-resolved in both the impurity-only and metoprolol-containing chromatograms. Relative peak areas in the impurity-only chromatogram were used as comparative expected values and were compared with the corresponding normalized relative areas in the metoprolol-containing chromatogram (Table S8). Normalization reduced the absolute integration error for several peaks, including peaks 3–5 integrated by ESM using IIS, whereas the magnitude of some other errors increased. Overall, however, the principal error patterns remained unchanged: large positive errors persisted for the co-eluting peaks with PDM, while ESM generally reduced these errors but showed variable performance across peaks and systems. Thus, normalization did not remove the overall differences observed between the integration approaches.

Taken together, the experimental results show that, in this selected small-molecule model system, integration of minor impurities eluting on the descending tail of a dominant metoprolol peak can result in substantial integration errors. PDM produced large positive errors for several co-eluting impurities, whereas ESM reduced the errors in many cases but did not provide uniformly accurate results. The amount and type of analyst interaction also varied between the evaluated commercial CDS workflows. The IIS results further indicate that automated processing alone does not guarantee small integration errors when the selected integration algorithm does not adequately account for the peak geometry. These findings are limited to the experimental conditions investigated here and should not be interpreted as a general assessment of routine QC performance.

5. Conclusions

In this study, we evaluated integration errors and analyst interaction associated with rule-based chromatographic peak-integration methods in selected pharmaceutical LC–UV impurity-analysis scenarios. Synthetic chromatograms with known input peak areas were combined with experimental metoprolol LC–UV data to assess integration performance across selected peak geometries and chromatographic conditions. The results showed that integration accuracy depended strongly on peak geometry, integration method, and software implementation, particularly when minor peaks occurred as shoulders or rider peaks on the tail of a dominant asymmetric peak.

For the selected baseline-resolved and partially overlapping symmetric peak configurations, PDM generally produced relatively small integration errors. The addition of baseline noise increased the errors in some cases, but the evaluated PDM implementations remained within approximately ±6.5%. Under these symmetric conditions, skimming did not provide a consistent numerical advantage over PDM.

Substantially larger errors were observed for several minor peaks in the selected asymmetric, shoulder, and rider-peak configurations. PDM produced particularly large positive errors for rider peaks superimposed on a sloping dominant-peak tail, including extreme errors exceeding several hundred percent in the selected synthetic rider-peak case. ESM substantially reduced the error for many individual rider peaks but did not provide uniformly accurate results across all peaks and systems. For shoulder configurations without a clearly defined valley, both peak detection and peak-area integration were sensitive to the specific processing approach, and neither PDM nor ESM provided consistently accurate results.

The experimental metoprolol model system showed related integration behavior in the presence of experimental noise, gradient elution, and co-elution on the descending metoprolol signal. PDM produced large positive errors for several co-eluting impurities, whereas ESM reduced these errors in many cases but did not eliminate them consistently. Because the impurity-only chromatogram provides a comparative reference rather than absolute ground truth, and replicate measurements were not used to quantify run-to-run variability, the experimental error estimates should be interpreted more cautiously than those obtained from the synthetic datasets. Normalization to a baseline-resolved reference peak reduced some individual errors but did not alter the principal error patterns.

The commercial CDS results also demonstrate that obtaining the reported analyst-optimized outcomes required varying degrees and types of analyst interaction. Click counts and numerical parameter inputs differed among chromatograms, integration methods, and software workflows. These metrics should be regarded as descriptive measures of analyst interaction rather than as direct measures of chromatographic difficulty, processing time, user effort, or comparative platform performance. The present study did not assess inter-analyst variability; workflows requiring greater analyst intervention may, however, provide greater opportunity for user-dependent outcomes.

Taken together, the findings indicate that no single evaluated rule-based integration approach provided uniformly accurate peak-area estimates across all of the selected peak geometries. PDM performed well in several symmetric cases but could produce very large errors for minor peaks on asymmetric or sloping backgrounds. ESM often improved rider-peak integration but remained dependent on the specific peak geometry and implementation. Similarly, automated processing without external user-tunable parameters did not by itself guarantee small integration errors when the selected integration algorithm did not adequately account for the peak geometry.

These results highlight the importance of selecting and controlling integration procedures according to the chromatographic peak configuration encountered. More robust integration strategies that account for asymmetry, tailing, partial overlap, and shoulder or rider-peak configurations while minimizing unnecessary analyst interaction may improve the consistency of impurity peak-area estimation. The conclusions are limited to the selected simulated and experimental conditions investigated here and should not be interpreted as a general comparison of CDS platforms or as an assessment of routine pharmaceutical QC performance.

CRediT authorship contribution statement

Martin Enmark: Writing – review & editing, Writing – original draft, Methodology, Investigation, Formal analysis, Data curation, Conceptualization. **Eivor Örnskov:** Writing – original draft, Resources, Methodology, Investigation, Formal analysis, Conceptualization. **Patrik Forssén:** Visualization, Software, Methodology, Data curation, Conceptualization. **Jörgen Samuelsson:** Writing – review & editing, Writing – original draft, Supervision, Methodology, Conceptualization. **Torgny Fornstedt:** Writing – review & editing, Writing – original draft, Supervision, Methodology, Funding acquisition, Conceptualization.

Funding

This work was supported by the Swedish Knowledge Foundation via the project "Improved Methods for Process and Quality Controls using Digital Tools" [grant number 20210021]. The funding source had no involvement in the study design; in the collection, analysis, or interpretation of data; in the writing of the report; or in the decision to submit the article for publication.

Declaration of Competing Interest

The authors have no known competing financial interests or personal relationships that could have appeared to influence the work reported in this paper.

Appendix A. Supporting information

Supplementary data associated with this article can be found in the online version at doi:10.1016/j.jpba.2026.117740.

Data Availability

The synthetic chromatograms can be reproduced from the models described in Section 2 and from the peak, noise, and system parameters given in the article and the Supplementary Material (Tables S1–S3). The processed integration results for the experimental data are reported in the article (Table 3) and the Supplementary Material (Tables S7 and S8). The raw experimental LC–UV chromatograms are publicly available at https://doi.org/10.5281/zenodo.22307140.

References

[1] N. Dyson. Chromatographic Integration Methods, 2nd ed., Royal Society of Chemistry, Cambridge, 1998.
[2] R.D. McDowall, Are you controlling peak integration to ensure data integrity? LCGC North Am. 38 (2020) 346–354.
[3] J.W. Dolan, Integration problems, LCGC North Am. 27 (2009) 892–899.
[4] N. Dyson, Peak distortion, data sampling errors and the integrator in the measurement of very narrow chromatographic peaks, J. Chromatogr. A 842 (1999) 321–340, https://doi.org/10.1016/S0021-9673(99)00299-X.
[5] International Council for Harmonisation (ICH), ICH Q2(R2): Validation of Analytical Procedures, 2023.
[6] International Council for Harmonisation (ICH), ICH Q6A: Specifications—Test Procedures and Acceptance Criteria for New Drug Substances and New Drug Products, 1999.
[7] International Council for Harmonisation (ICH), ICH Q3A(R2): Impurities in New Drug Substances, 2006.
[8] International Council for Harmonisation (ICH), ICH Q3B(R2): Impurities in New Drug Products, 2006.
[9] Parenteral Drug Association (PDA), Technical Report No. 80: Data Integrity Management System for Pharmaceutical Laboratories, PDA, Bethesda, MD, 2018.
[10] U.S. Food and Drug Administration, Center for Drug Evaluation and Research, Warning Letter Glenmark Pharmaceuticals Limited, MARCS-CMS 637314, 2022. https://www.fda.gov/inspections-compliance-enforcement-and-criminal-investigations/warning-letters/glenmark-pharmaceuticals-limited-637314-11222022 (accessed 20 February 2026).
[11] U.S. Food and Drug Administration, Center for Drug Evaluation and Research, Warning Letter Intas Pharmaceuticals Limited, MARCS-CMS 662868, 2023. https://www.fda.gov/inspections-compliance-enforcement-and-criminal-investigations/warning-letters/intas-pharmaceuticals-limited-662868-11212023 (accessed 20 February 2026).
[12] M.K.L. Bicking, Integration errors in chromatographic analysis, Part I: Peaks of approximately equal size, LCGC North Am. 24 (2006) 402–414.
[13] M.K.L. Bicking, Integration errors in chromatographic analysis, Part II: Large peak size ratios, LCGC North Am. 24 (2006) 604–616.
[14] V.R. Meyer, Errors in the area determination of incompletely resolved chromatographic peaks, J. Chromatogr. Sci. 33 (1995) 26–33.
[15] V.R. Meyer, Quantitation of chromatographic peaks in the 0.1–1.0% range, Chromatographia 40 (1995) 15–22.
[16] R.D. McDowall, Data Integrity and Data Governance: Practical Implementation in Regulated Laboratories, Royal Society of Chemistry, Cambridge, 2018, https://doi.org/10.1039/9781788013277.
[17] S. Jurt, M. Schär, V.R. Meyer, Procedure for the quantification of rider peaks, J. Chromatogr. A 929 (2001) 165–168, https://doi.org/10.1016/S0021-9673(01)01164-5.
[18] C. Bueschl, M. Doppler, E. Varga, B. Seidl, M. Flasch, B. Warth, J. Zanghellini, PeakBot: machine-learning-based chromatographic peak picking, Bioinformatics 38 (2022) 3422–3428, https://doi.org/10.1093/bioinformatics/btac344.
[19] T. Blanc, H. Wätzig, C. Sänger-van de Griend, Peak Integration of Electropherograms in GMP and Research Labs: Navigating Increased Scrutiny Amid Data Integrity Audits and Inspections, Electrophoresis 46 (2025) 653–668, https://doi.org/10.1002/elps.70002.
[20] P. Forssén, T. Fornstedt, Accuracy of methods for integrating overlapping chromatographic peaks: A systematic evaluation, J. Chromatogr. A 1787 (2026) 467393, https://doi.org/10.1016/j.chroma.2026.467393.
[21] F. Liu, Safety assessment of drug impurities for patient safety: A comprehensive review, Regul. Toxicol. Pharmacol. 153 (2024) 105715, https://doi.org/10.1016/j.yrtph.2024.105715.
[22] P. Borman, D. Elder, Q2(R1) Validation of Analytical Procedures: Text and Methodology, in: A. Teasdale, D. Elder, R.W. Nims (Eds.), ICH Quality Guidelines: An Implementation Guide, John Wiley & Sons, Hoboken, NJ, 2017, pp. 127–166, https://doi.org/10.1002/9781118971147.ch5.
[23] J. Ermer, Validation in pharmaceutical analysis. Part I: An integrated approach, J. Pharm. Biomed. Anal. 24 (2001) 755–767, https://doi.org/10.1016/S0731-7085(00)00530-6.
[24] J. Peris-Vicente, J. Esteve-Romero, S. Carda-Broch, Validation of Analytical Methods Based on Chromatographic Techniques: An Overview, in: V. Pino, J. L. Anderson, A. Berthod, A.M. Stalcup (Eds.), Analytical Separation Science, Wiley-VCH, Weinheim, 2015, pp. 1757–1808, https://doi.org/10.1002/9783527678129.assep064.
[25] Q. Xu, Advancing USP compendial methods for fixed dose combinations: A case study of metoprolol tartrate and hydrochlorothiazide tablets, J. Pharm. Anal. 9 (2019) 77–82, https://doi.org/10.1016/j.jpha.2018.12.003.
[26] Y. Liu, J. Lin, A general-purpose signal processing algorithm for biological profiles using only first-order derivative information, BMC Bioinforma. 20 (2019) 611, https://doi.org/10.1186/s12859-019-3188-4.
[27] M. Schmid, D. Rath, U. Diebold, Why and how Savitzky–Golay filters should be replaced, ACS Meas. Sci. Au 2 (2022) 185–196, https://doi.org/10.1021/acsmeasuresciau.1c00054.
[28] PeakLab Software, version 1.0, AIST Software Inc., Mapleton, OR, USA, September 2022.
[29] G. Guiochon, A. Felinger, D.G.G. Shirazi. Fundamentals of Preparative and Nonlinear Chromatography, 2nd ed., Academic Press, Boston, 2006.
[30] O. Gyllenhaal, J. Vessman, Potential of packed column supercritical fluid chromatography for the separation of metoprolol from closely related compounds, J. Chromatogr. A 839 (1999) 141–148, https://doi.org/10.1016/S0021-9673(99)00052-7.
[31] A. Felinger, M. Káré, Wavelet analysis of the baseline noise in HPLC, Chemom. Intell. Lab. Syst. 72 (2004) 225–232, https://doi.org/10.1016/j.chemolab.2004.01.018.